

Electron Density and Dipole Moment Analysis of Valence-Electron Wave Functions

Donald B. Boyd

Contribution from The Lilly Research Laboratories, Eli Lilly and Company, Indianapolis, Indiana 46206. Received May 8, 1971

Abstract: A comparison of the electronic structure of adenine, as described by three different molecular orbital methods, is given in terms of electron density maps and dipole moment partitioning. The valence-electron wave functions are computed by the extended Hückel (EH), complete neglect of differential overlap (CNDO/2), and CNDO deorthogonalized (CNDO/2D) methods. The exaggeration of net atomic charges by the EH method is reflected in a large point-charge dipole moment and in the spatial disposition of electrons. Deorthogonalization by a Löwdin transformation of the CNDO/2 LCAO-MO coefficients shifts σ and π electrons away from the atoms and into the bonding and lone-pair regions. Dipole moments partitioned by Ruedenberg's origin-invariant method indicate that atomic and bond moment components partially offset each other in adenine, contributing to a similarity of the point charge and rigorous total dipole moments. Knowledge gained from this analysis on the electronic structure of adenine has application in the study of the chemical and physical properties of adenine in biological systems.

Characterizations of the all-valence-electron molecular orbital theories popular for the study of large molecules have been in terms of aggregate properties of electronic structure. For instance, the extended Hückel (EH) and complete neglect of differential overlap (CNDO/2) methods have been compared on the basis of population analyses, ionization potentials, dipole moments, conformations, and other structural features predicted by the methods.¹ These properties depend wholly or partially on the total gross electronic distribution and do not reveal much information about the detailed way in which electrons are distributed in space around the nuclear skeleton of a molecule.

Detailed information can be obtained from two approaches. One is the Ruedenberg origin-invariant method of partitioning the total molecular dipole moment into a point-charge term, atomic moments computed with one-center density matrix elements, and bond moments computed with the two-center matrix elements.² The point-charge term is just the classical moment based on net atomic charges. An atomic moment is a local dipole moment associated with the asymmetric arrangement of charge in the orbitals of a given atom, and the bond moment is due to the apportionment of charge between the orbitals of a pair of atoms within the molecule.

The second approach for a detailed analysis of electronic structure is to compute electron density maps.³ Such contour diagrams can show for any plane through a molecule the concentration of all or only some of the electrons in that plane. Plots can also be made of the difference between the molecular and composite atomic densities to show the effects of molecular formation. Alternatively, plots of the difference in density between two wave functions of the same molecule can

show the effects of the basis functions or various approximations entering into the solution of the wave function.

Although most research with electron density maps has involved *ab initio* wave functions, the analyses of valence-electron wave functions have had their place.⁴⁻⁸ In the earliest publication, the rearrangements of electrons during the course of nucleophilic attack were mapped.⁴ The nature of the phosphorus-carbon double bond and the unusual participation of P 3d orbitals in alkylidene phosphoranes have been elucidated with density difference maps.⁵ Also, the ability of 3d orbitals to enter into stronger $d_{\pi}-p_{\pi}$ bonding in the terminal P-O bonds of ATP than in the bridging, pyrophosphate P-OP bonds was illustrated⁶ as an intramolecular effect determining to some extent⁹ the free energy of hydrolysis and transfer potential of ATP. The semiempirical density distributions can at best only qualitatively mimic *ab initio* and true distributions.⁶ Of course, this is partly related to the fact that polarizations of the core electrons, while usually small,^{3,10} are altogether neglected. Nevertheless, we emphasize that the purpose of this paper is not to emulate *ab initio* results, but rather to compare the semiempirical wave functions with each other and thereby to understand the characteristics of the valence-electron theories better.

We choose to treat adenine. The planarity of this molecule allows separate or simultaneous examination of the σ and π electrons, even though, of course, the wave functions are obtained by treating all valence electrons simultaneously. Adenine is biologically important and is one of the most frequently studied large

(1) See, e.g., (a) A. Pullman in "Quantum Aspects of Heterocyclic Compounds in Chemistry and Biochemistry," E. D. Bergmann and B. Pullman, Ed., Academic Press, New York, N. Y., 1970, p 9; A. Pullman, *Ann. N. Y. Acad. Sci.*, **158**, 65 (1969); (b) J. R. Hoyland in "Molecular Orbital Studies in Chemical Pharmacology," L. B. Kier, Ed., Springer-Verlag, New York, N. Y., 1970, p 31.

(2) K. Ruedenberg, *Rev. Mod. Phys.*, **34**, 326 (1962).

(3) D. B. Boyd, *J. Chem. Phys.*, **52**, 4846 (1970), and references therein.

(4) D. B. Boyd, *J. Amer. Chem. Soc.*, **91**, 1200 (1969).

(5) R. Hoffmann, D. B. Boyd, and S. Z. Goldberg, *ibid.*, **92**, 3929 (1970); D. B. Boyd and R. Hoffmann, *ibid.*, **93**, 1064 (1971).

(6) D. B. Boyd, *Theor. Chim. Acta*, **18**, 184 (1970).

(7) R. B. Hermann, H. W. Culp, R. E. McMahon, and M. M. Marsh, *J. Med. Chem.*, **12**, 749 (1969).

(8) G. Colombetti and C. Petrongolo, *Theor. Chim. Acta*, **20**, 31 (1971); O. Martensson and G. Sperber, *Acta Chem. Scand.*, **24**, 1749 (1970).

(9) Solvation will also have an effect on a solution-phase reaction, yet even solvation energies are a function of the electronic properties of the solute molecules.

(10) D. B. Boyd, *Theor. Chim. Acta*, **20**, 273 (1971).

molecules. Moreover, *ab initio* calculations with small and large basis sets of Gaussian-type orbitals have been performed on adenine.¹¹ A direct numerical comparison of the valence-electron and *ab initio* results would not be prudent because of the recognized dependence of electron density on the basis set.^{3,12} The maps we present, however, should serve for qualitative, visual comparison when the *ab initio* wave functions are fully analyzed.¹³

Method and Theory

Three all-valence-electron methods will be used to obtain the wave functions for adenine: (1) EH,¹⁴ (2) CNDO/2,¹⁵ and (3) CNDO/2D.^{16,17} The parameters entering the EH and CNDO/2 calculations have been published,^{14,15} and the molecular geometry adopted is described in a preliminary account of this work.¹⁸ The CNDO/2D method entails a deorthogonalization procedure which renormalizes the CNDO/2 LCAO-MO coefficient matrix with a Löwdin transformation, $C' = S^{-1/2}C$, (where S is overlap matrix) and which also removes the approximation of neglect of differential overlap.

To understand the relation of the CNDO/2 and CNDO/2D wave functions, note that the basis set in the standard CNDO/2 framework can be regarded from two viewpoints. One is that the basis set consists of Slater-type functions, and their nonorthogonality is then disregarded *via* the approximation of neglect of differential overlap. The second is that the CNDO/2 method is fashioned in terms of orthogonalized atomic orbitals, and then certain integrals are approximated *via* the corresponding integrals over Slater-type functions. Whereas both viewpoints may have their validity, we prefer and will use the former. Support for this viewpoint is contained both in the original papers of Pople^{15,19} and in the name CNDO itself (as contrasted with some acronym based on linear combinations of orthogonalized atomic orbitals). Considering the Slater-type basis set then, we see that the deorthogonalization procedure can be rationalized as both a renormalization of the LCAO-MO coefficients and a removal of the approximation of neglect of differential overlap. Thus, our deorthogonalization process is not simply an orthogonal transformation which leaves the wave function invariant. Instead, it creates a new wave function to be treated without

neglect of differential overlap in the same manner which has been discussed by others.^{16,17}

It is sometimes overlooked that zero or complete neglect of differential overlap²⁰ entails setting the product of two different basis functions equal to zero, $\chi_p\chi_q = 0$, and then from this it follows that $S_{pq} = \delta_{pq}$. Ordinarily, one invokes the approximation of neglecting the overlap of different basis functions in only some of the steps of solving the CNDO/2 wave function, and it is sufficient to think of the approximation as applying only to integrals. However, when one wishes to compute electron densities, it becomes necessary to recall the fundamental meaning of the approximation. In the next few paragraphs, we will see how this approximation enters into the dipole moment and electron density calculations.

In the Ruedenberg scheme² for dipole moment partitioning, the net atomic charge of each atom A is defined according to Mulliken²¹ as

$$Q(A) = - \sum_p^A \sum_q^{\text{all}} D_{pq} S_{pq} + Z_A \quad (1)$$

where the density matrix elements are obtained by summing products of the LCAO-MO coefficients over all N valence electrons

$$D_{pq} = \sum_{i=1}^N C_{pi} C_{qi}$$

S_{pq} is the overlap integral between two Slater-type orbital basis functions, and Z_A is the core charge on atom A. The first sum in eq 1 is over all basis functions on center A, and the second sum is over all basis functions in the molecule. From $Q(A)$, the point-charge moment in the x direction is found from

$$\mu_{PTQ}(x) = \sum_A \sum_p^A \sum_q^{\text{all}} D_{pq} S_{pq} X_A - \sum_A Z_A X_A \quad (2)$$

where X_A is the Cartesian coordinate of atom A (analogous expressions hold for the y and z directions). In our equations atomic units (1 au = 2.54158 D) and the usual chemical convention for dipole moment direction (+ to -) are employed. The atomic moment for each atom A is given by

$$\mu_A(x) = 2 \sum_p^A \sum_{q < p}^A D_{pq} [\mu_{pq}^{x(\text{mol})} - S_{pq} X_A] \quad (3)$$

where the dipole moment integral $\mu_{pq}^{x(\text{mol})}$ is computed in the molecular coordinate system. Translation of the coordinate system origin to atom A replaces the quantity in brackets by simply $\mu_{pq}^{x(A)}$. The bond moment, despite its name, is evaluated for all pairs of atoms in the molecule

$$\mu_{AB}(x) = 2 \sum_p^A \sum_q^B D_{pq} [\mu_{pq}^{x(\text{mol})} - \frac{1}{2} S_{pq} (X_A + X_B)] \quad (4)$$

If the origin is at the midpoint of the line connecting atoms A and B, the quantity in the brackets reduces to $\mu_{pq}^{x(\text{midpoint})}$, which is the integral evaluated from the midpoint. The total dipole moment is the sum of μ_{PTQ} , μ_A added over all atoms, and μ_{AB} added over all distinct atom pairs.

(11) B. Mély and A. Pullman, *Theor. Chim. Acta*, **13**, 278 (1969); E. Clementi, J. M. André, M. C. André, D. Klint, and D. Hahn, *Acta Phys. Acad. Sci. Hung.*, **27**, 493 (1969).

(12) C. W. Kern and M. Karplus, *J. Chem. Phys.*, **40**, 1374 (1964); K. E. Banyard and M. R. Hayns, *J. Phys. Chem.*, **75**, 416 (1971).

(13) A. Pullman, M. Dreyfus, and B. Mély, *Theor. Chim. Acta*, **17**, 85 (1970), have reported only total density maps of their wave function.

(14) D. B. Boyd and W. N. Lipscomb, *J. Theor. Biol.*, **25**, 403 (1969), and references therein.

(15) J. A. Pople and G. A. Segal, *J. Chem. Phys.*, **44**, 3289 (1966).

(16) C. Giessner-Prettre and A. Pullman, *Theor. Chim. Acta*, **11**, 159 (1968).

(17) D. D. Shillady, F. P. Billingsley, and J. E. Bloor, *ibid.*, **21**, 1 (1971).

(18) D. B. Boyd, Proceedings of the Jerusalem Symposium on Quantum Chemistry and Biochemistry, April 5-9, 1971, E. D. Bergmann and B. Pullman, Ed., Academic Press, New York, N. Y., in press. This paper also reports the evaluation of the dipole moment integrals and the Ruedenberg partitioning of the dipole moments of some second-row hydrides and diatomics.

(19) J. A. Pople, D. P. Santry, and G. A. Segal, *J. Chem. Phys.*, **43**, S129 (1965); J. A. Pople and G. A. Segal, *ibid.*, **43**, S136 (1965).

(20) R. Pariser and R. G. Parr, *ibid.*, **21**, 466 (1953).

(21) R. S. Mulliken, *ibid.*, **23**, 1833 (1955).

$$\mu_{\text{tot}}(x) = \mu_{\text{PTQ}}(x) + \sum_A \mu_A(x) + \sum_{A < B} \mu_{AB}(x) \quad (5)$$

For a neutral molecule, the partitions and the total dipole moment are invariant to a shift of origin.

With the EH and CNDO/2D wave functions, where the basis sets are logically treated as being nonorthogonal, eq 1-5 may be used as given with the exactly evaluated integrals. On the other hand, in the CNDO/2 framework, the molecular orbitals are normalized subject to the assumption of orthogonal basis functions. Thus, in the standard CNDO procedure^{15,19} the overlap integrals are taken as $S_{pq} = \delta_{pq}$, and only the one-center dipole moment integrals are retained. The CNDO/2 procedure follows directly from the Ruedenberg analysis when in eq 1-5 the unit matrix is used in place of the overlap matrix and the bond moments (eq 4) are neglected altogether. Note that the retention of the atomic moments (\mathbf{y}_{sp} in CNDO/2 notation and the second term of eq 5 in our notation) is advantageous because the point-charge moments are in rather poor agreement with experiment and the atomic moments generally correct them in the proper direction.^{19,22}

We will be presenting two types⁵ of electron density difference maps, which, as we have shown,^{3,6,10} are more informative and of greater chemical interest than plots of the total density from a valence-electron wave function. One type of difference map (molecular minus atomic) shows the difference between the molecular density and that due to the superimposed densities of the constituent atoms placed in the nuclear geometry of the molecule. The relevant difference function for points in space \mathbf{r} is

$$\Delta D(\mathbf{r}) = \sum_{p,q \neq p}^{\text{all}} D_{pq} \chi_p(\mathbf{r}) \chi_q(\mathbf{r}) + \sum_p^{\text{all}} [D_{pp} - N(p)] \chi_p(\mathbf{r}) \chi_p(\mathbf{r}) \quad (6)$$

where the χ_p 's are the Slater-type basis functions with the standard exponents employed in the EH and CNDO/2 methods. The D_{pq} 's are density matrix elements computed from the molecular wave function, but in the CNDO/2 formulation the off-diagonal density matrix elements and hence the first term of eq 6 are dropped by neglect of differential overlap, just as in the calculation of the total atomic charges.¹⁵ The $N(p)$'s of eq 6 are occupation numbers of the valence atomic orbitals in the reference state. This reference state is ordinarily the neutral, spherically symmetric, ground state of each atom. For instance, $N(\text{H } 1s)$ is 1, $N(\text{C } 2s)$ and $N(\text{N } 2s)$ are 2, and $N(\text{C } 2p)$ and $N(\text{N } 2p)$ are $2/3$ and 1, respectively, for each p orbital. Equation 6 and the use of these $N(p)$'s follow from the desire to have the atomic densities correspond to the same level of approximation as the molecular density.^{3,6,23} When $\Delta D(\mathbf{r})$ as just described is integrated over all space, zero is obtained. However, we also include maps of what happens to the π -electron cloud. For these maps a different reference state is chosen: all carbons and nitrogens are regarded as donating one

(22) Various levels of approximation, as determined by which Ruedenberg components are retained or neglected, have been investigated for several types of wave functions in ref 16.

(23) The relation of the total molecular density to the Mulliken orbital occupation numbers of the molecule (rather than the atoms) has been analyzed in ref 6.

electron to the π -electron system, except N_9 and N_{10} which donate two each. By this choice of $N(\text{N } 2p_\pi)$, the property of having $\Delta D(\mathbf{r})$ integrate to zero is maintained.

The second type of density difference map (molecular minus molecular) contrasts the density computed from two different wave functions associated with density matrices \mathbf{D}' and \mathbf{D}'' , respectively. Hence we use

$$\Delta D(\mathbf{r}) = \sum_{p,q}^{\text{all}} D_{pq}' \chi_p(\mathbf{r}) \chi_q(\mathbf{r}) - \sum_{r,s}^{\text{all}} D_{rs}'' \chi_r(\mathbf{r}) \chi_s(\mathbf{r}) \quad (7)$$

where the basis sets in the two wave functions happen to be the same because of the way the EH, CNDO/2, and CNDO/2D methods are formulated. In the case of comparison with a CNDO/2 wave function, a neglect of all off-diagonal contributions must be made in the corresponding term of eq 7 because of the neglect of differential overlap approximation.

Dipole Moments

In this section we intend to show that the Ruedenberg analysis of dipole moments provides a very detailed picture of electronic structure and clarifies various approximations and contributions entering into the calculations. We also examine the effect of deorthogonalization and the polarity of adenine as given by different theories. The net atomic charges used in computing μ_{PTQ} are given in Table I. For most atoms,

Table I. Net Atomic Charges in Adenine^a

Atom	EH	CNDO/2D	CNDO/2
N ₁	-0.86	-0.32	-0.30
C ₂	+0.56	+0.25	+0.22
H ₂	+0.02	-0.01	-0.03
N ₃	-0.75	-0.29	-0.25
C ₄	+0.47	+0.26	+0.20
C ₅	+0.08	-0.00	-0.05
C ₆	+0.58	+0.32	+0.27
N ₁₀	-0.30	-0.40	-0.22
H ₁₀	+0.21	+0.18	+0.13
H _{10'}	+0.21	+0.18	+0.12
N ₇	-0.81	-0.23	-0.19
C ₈	+0.46	+0.19	+0.15
H ₈	+0.05	+0.02	-0.01
N ₉	-0.13	-0.32	-0.15
H ₉	+0.21	+0.17	+0.11

^a The atomic numbering system is shown in Figure 1.

the CNDO/2D charges are intermediate between the EH and CNDO/2 values.

The atomic dipole moment vectors (Figure 1) are associated with the asymmetric distribution of electrons among the orbitals of each atom and thus are large for the atoms with lone pairs and zero for the hydrogens. The imine nitrogens, which carry the large lone-pair vectors, are those involved in hydrogen bonding and other electron-donor interactions.²⁴ The CNDO/2 and EH atomic moments are actually quite similar. On the other hand, deorthogonalization has greatly increased the atomic moments, especially for N_1 , N_3 , and N_7 . No one MO makes a dominant contribution to the lone pairs on these atoms, and, in fact, the expectation values of position for the occupied MO's of

(24) See, e.g., D. Voet and A. Rich, *Progr. Nucl. Acid Res. Mol. Biol.*, **10**, 183 (1970); E. Sletten, *Acta Crystallogr., Sect. B*, **25**, 1480 (1969).

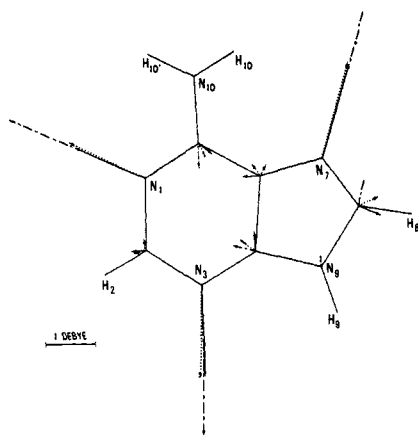


Figure 1. Atomic moments (D) of adenine from EH (—), CNDO/2D (---), and CNDO/2 (····) wave functions. Each atomic moment vector has been translated to originate at its respective atom. Some atomic moments are too small to draw at the scale used; the relation of the distance scale to the dipole moment scale is arbitrary.

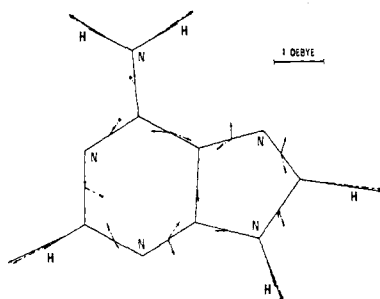


Figure 2. Bond moments (D) from EH (—) and CNDO/2D (---) wave functions. Origin of the vectors for each pair of bonded atoms was selected as the midpoint of that bond.

all three wave functions fall in a cluster near the center of the molecule.

Values of μ_{AB} , where A and B are covalently bonded atoms, are depicted in Figure 2. Only the C-H and N-H bonds have large bond moments, and these are similar in both procedures where they are included (EH and CNDO/2D). Charge distributions between the other atoms are seen to be more or less randomly polarized. Values of μ_{AB} for nonbonded atoms are generally smaller than those depicted.

Summarized in Figure 3 are the resultant dipole moment partitions and the total dipole moment vectors. Values of μ_{tot} are also presented in Table II

Table II. Summary of Dipole Moment Lengths (D) and Directions^a

	EH	CNDO/2D	CNDO/2
$\mu_{tot}(\sigma)$	0.95 (59°)	0.07 (149°)	0.52 (52°)
$\mu_{tot}(\pi)$	3.49 (96°)	1.93 (92°)	1.90 (94°)
$\mu_{tot}(\sigma + \pi)$	4.29 (88°)	1.97 (94°)	2.32 (85°)

^a Angles measured counterclockwise from the line connecting N_3 at the origin to C_6 .

with a breakdown into σ and π electrons. No experimental data have been obtained for unsubstituted adenine, although the dipole moment is generally

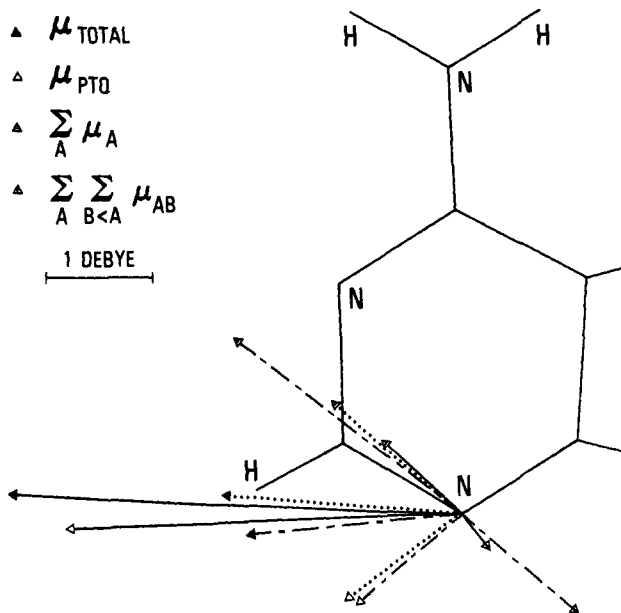


Figure 3. Resultant dipole moment vectors (D) of adenine from EH (—), CNDO/2D (---), and CNDO/2 (····) wave functions. Molecular origin is at N_3 .

assumed to be near 3 D as found for 9-*n*-butyladenine.²⁵ Most quantum mechanically calculated dipole moments of adenine have fallen in the range 2–4 D (see ref 1a and 18, and references therein) with the direction from the imidazole ring toward the pyrimidine ring as we find. By our calculations (Table II) and *ab initio* calculations,¹⁸ the dipole moment is determined to a large extent by the 12 electrons making up the π -electron system. The π dipole moments are computed using the core charges as commonly employed in π -electron theory, whereas the σ moments are based on the 38 electrons in the σ MO's and the remaining core charges. Deorthogonalization does not affect the π dipole moments significantly, which coincides with previous findings^{16,17} that the $S^{-1/2}$ transformation mixes the σ LCAO-MO coefficients more strongly. However, we will see later that the renormalization to a nonorthogonal basis and removal of the neglect of differential overlap approximation do not leave the π electrons unscathed. Deorthogonalizing has no advantageous effect on bringing the CNDO/2 μ_{tot} into better agreement with experiment. Giessner-Prettre and Pullman¹⁶ reached a similar conclusion, and Bloor and co-workers¹⁷ found CNDO/2D only marginally better than CNDO/2 for the compounds they studied.

As seen in Figure 3, each type of resultant moment (point charge, atomic, and bond) is roughly in the same direction regardless of the valence-electron method. The lengths of the vectors do vary with the method. The EH molecular orbitals, for instance, are known to exaggerate net atomic charges (Table I), and this is reflected in the long μ_{PTQ} vector. The μ_{PTQ} vectors from CNDO/2D and CNDO/2 are shorter and almost coincide. As with the individual atomic moments (Figure 1), the resultant atomic moments reveal the biggest effect of deorthogonalization: the CNDO/2D

(25) H. DeVoe and I. Tinoco, Jr., *J. Mol. Biol.*, **4**, 500 (1962). This paper is frequently incorrectly quoted in regard to the experimental dipole moment of 9-methyladenine.

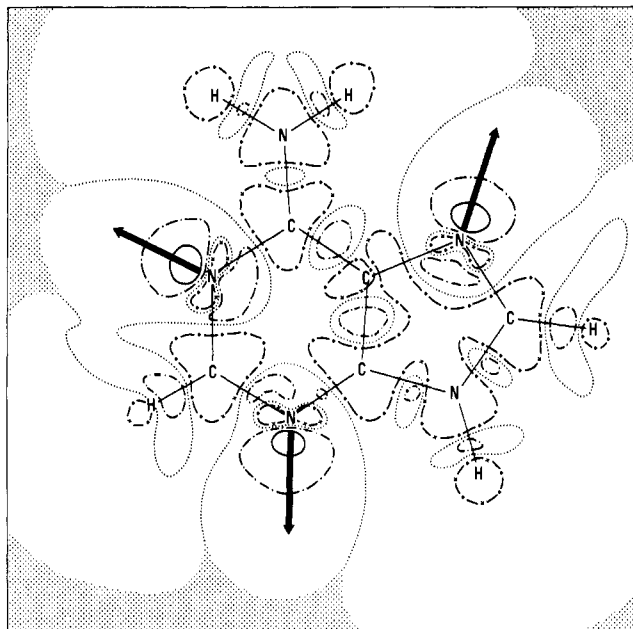


Figure 4. EH molecular-minus-atomic difference map. Contours are at $+0.155$ e/bohr³ (—), $+0.019$ (-·-), and -0.019 (-×-). 1 e/bohr³ = 6.749 e/Å³. Scale for μ_A is arbitrary.

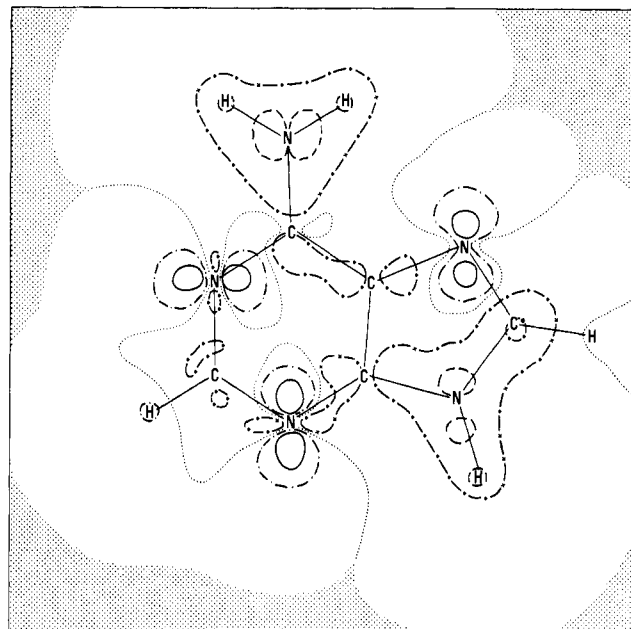


Figure 6. CNDO/2 molecular-minus-atomic difference map. Contours are at $+0.042$ e/bohr³ (—), -0.042 (- - -), $+0.010$ (-·-), and -0.010 (-×-).

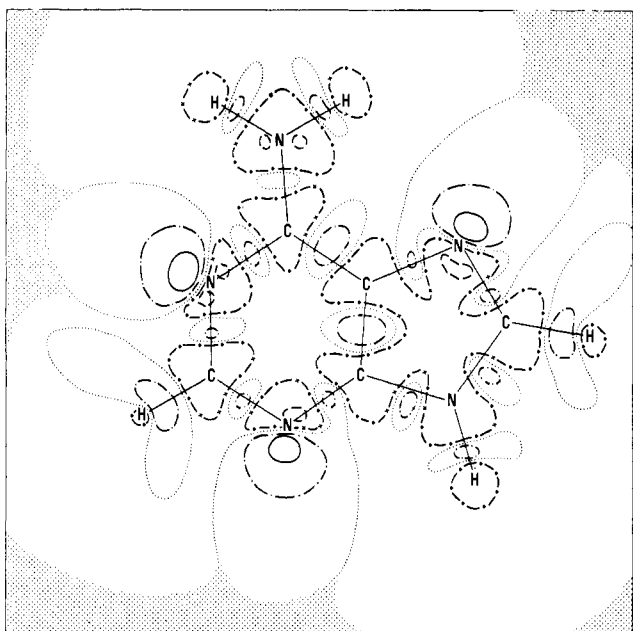


Figure 5. CNDO/2D molecular-minus-atomic difference map. Contours are at $+0.132$ e/bohr³ (—), -0.132 (- - -), $+0.017$ (-·-), and -0.017 (-×-).

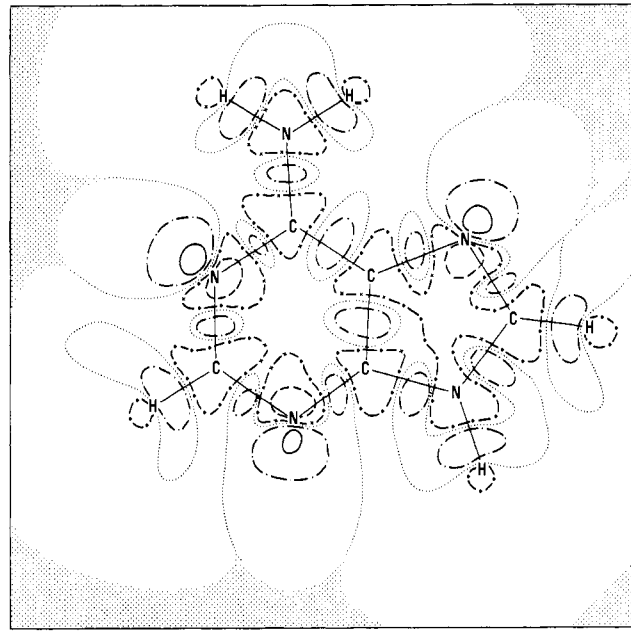


Figure 7. CNDO/2D-minus-CNDO/2 difference map of adenine. Contours are at $+0.113$ e/bohr³ (—), -0.113 (- - -), $+0.014$ (-·-), and -0.014 (-×-).

$\Sigma_A \mu_A$ is much larger than the CNDO/2 value. This increase is partially offset by the resultant bond moment which enters in the CNDO/2D procedure. Based on the μ_{PTQ} 's alone, the CNDO/2 and CNDO/2D treatments suggest an electronic structure of adenine less polar than commonly accepted. However, the data of Figure 3 show that none of the Ruedenberg components may be regarded as negligible. The point-charge vector is a large factor in the determination of each total moment, but as should be recognized, close agreement of rigorous and point-charge moments is usually fortuitous.

Electron Density Maps

In the preceding section, we have examined one way in which to analyze electronic structure. Next we focus on the charge distribution at still finer resolution. Figures 4–8 present plots of various $\Delta D(\mathbf{r})$ as evaluated in the plane of the molecule. Nodes and regions where the density is less than 10^{-6} e/bohr³ are dotted. Atomic locations and internuclear axes indicate the scale of the figures (e.g., C_2-N_7 distance is 4.0294 Å).

Consider first the molecular-minus-atomic type of map computed from all MO's and spherical, reference atomic densities. The EH (Figure 4) and CNDO/2D

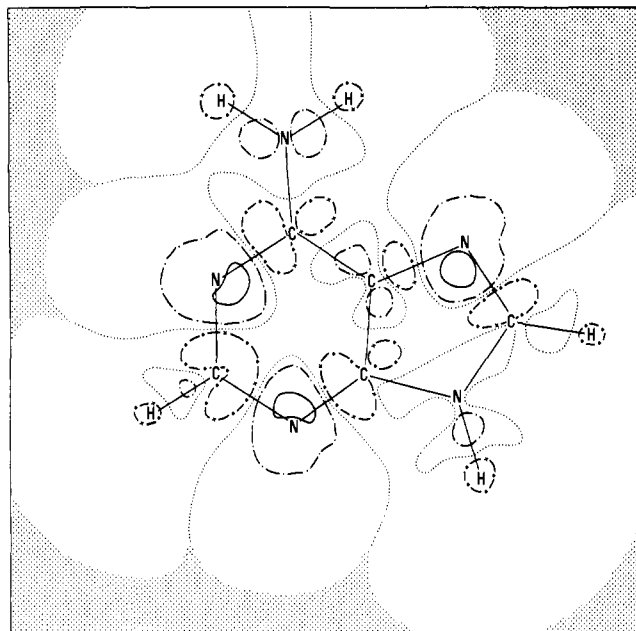


Figure 8. EH-minus-CNDO/2D difference map. Contours are at $+0.091 \text{ e/bohr}^3$ (—), $+0.011$ (- · -), and -0.011 (-x-).

(Figure 5) maps quite clearly show the accumulations of electrons at and along the internuclear axes and in lone-pair lobes on the imine nitrogens. The relation of the lone-pair regions to the ψ_A is also shown in Figure 4. The apparent sizes of the lone-pair lobes cannot be directly related to the net atomic charges (Table I) because the charge distribution on the other sides of these atoms must also be examined. It is gratifying that the EH and CNDO/2D maps are in harmony with chemical concepts on the formation of molecules from atoms, *i.e.*, they show greater probability of electrons in those regions associated with bonding and lone pairs. On the other hand, the CNDO/2 map (Figure 6) is strikingly dissimilar to Figures 4 and 5. This must be due to the neglect of the off-diagonal matrix terms of eq 6 as required in the CNDO/2 scheme. The CNDO/2 map shows only three regions of density gain, and these appear as in-plane 2p atomic orbitals of the imine nitrogens. Notice from the numerical values of the contours that the peaks and valleys of the EH map (Figure 4) are most pronounced and those of the CNDO/2 map are least pronounced. The leveling out of the charge distribution is related to the iterative process of obtaining the molecular orbitals in CNDO/2 theory.

A more direct comparison of the valence-electron wave functions is made by observing the molecular-minus-molecular difference maps of Figures 7 and 8. We have noted before with the net atomic charges (Table I) and Figures 4–6 that the CNDO/2D results appear to be intermediate between those from EH and CNDO/2 theory. The relation of the CNDO/2D and CNDO/2 densities is illustrated in Figure 7. Deorthogonalization shifts electron density away from each atom into the σ bonding regions along the internuclear axes as drawn and into the lone pair regions. Thus, the features associated with molecular formation are brought out. Figure 8 shows that the CNDO/2D distribution is not drastically different from the EH form. The EH wave function has more lone-pair density, associated presumably with the exaggeration

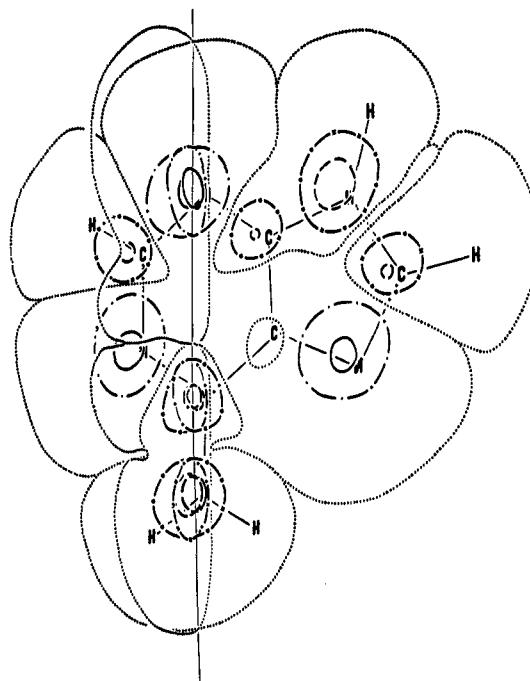


Figure 9. EH molecular-minus-atomic difference map for the π -electron system. Contours are at $+0.050 \text{ e/bohr}^3$ (—), -0.050 (- - -), $+0.010$ (- · -), and -0.010 (-x-).

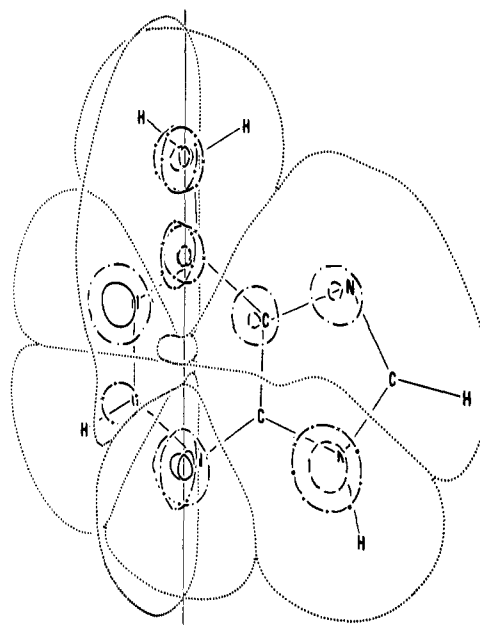


Figure 10. CNDO/2 molecular-minus-atomic difference map for the π -electron system. Contours are at $+0.040 \text{ e/bohr}^3$ (—), -0.040 (- - -), $+0.010$ (- · -), and -0.010 (-x-).

of charge. The larger EH lone pairs are not in conflict with the larger CNDO/2D atomic moments of the imine nitrogens because it can be noticed that the EH wave function also has more density on the back sides of these atoms. Recognizing the manner in which the population analysis²¹ divides charge between two atoms, one may observe in Figure 8 that C_2 , C_4 , C_6 , and C_8 should be more positive and N_1 , N_3 , and N_7 should be more negative in EH theory than in CNDO/2D theory, as indeed they are (Table I).

We have seen what happens to the σ electrons in Figures 4–8 since, after all, the π electrons cannot con-

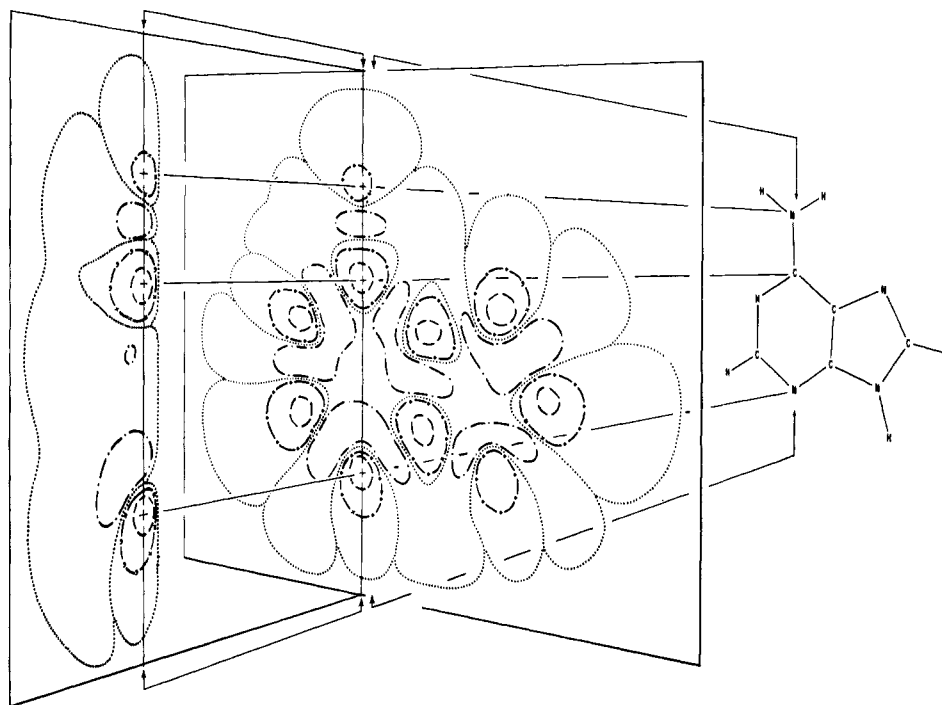


Figure 11. CNDO/2D-minus-CNDO/2 difference map for the π -electron system. Contours are at $+0.020$ e/bohr³ (—), -0.020 (---), $+0.002$ (· · ·), and -0.002 (-×-). The two maps lying in their respective planes have been separated in this perspective in order to avoid overlapping of the contour lines. The line of intersection of the two planes and the spatial relation of the maps to the structure of adenine are also indicated.

tribute to the density in the plane of the molecule. The density due to the π electrons maximizes about 0.2–0.6 Å above and below the molecular plane. But the σ electrons do have some probability at these distances. Hence we will compute $\Delta D(\mathbf{r})$ from only the six filled π MO's, and the density of the σ electrons will not interfere. Each of the π -electron figures contains two maps viewed in perspective and computed as described in the Method and Theory section. One map is of the plane parallel to the molecular plane and 0.4 Å above it. The second plane intersects the first at right angles and passes through atoms N₃ and C₆ and near the amino nitrogen N₁₀. The loci of intersection of the two planes are indicated by the vertical lines in the figures. Beyond the outer perimeter of dots in Figures 9–11, the difference function is less than 10^{-6} e/bohr³.

Figure 9 displays the rearrangement of the π electrons in EH theory with respect to the π -electron reference atomic state. As expected, the regions above N₉ and N₁₀ are depleted of electrons because these atoms are assumed to donate two electrons each to the π -electron system. Those atoms with lone pairs, N₁, N₃, and N₇, show gains in their $2p_{\pi}$ orbitals (as well as their in-plane orbitals, Figure 4). No gain in density is apparent in the perpendicular plane to indicate a C₆–N₁₀ π bond, contrasting with previously studied π bonding situations.^{5,6} The CNDO/2 map (Figure 10) shows features similar to those of Figure 9, although the $\Delta D(\mathbf{r})$ function varies through a smaller range because of the self-consistency of the CNDO/2 molecular orbitals. The CNDO/2D map is not reproduced here because it appears as a hybrid of Figures 9 and 10, the main differences being that, compared to the EH map, the CNDO/2D map has less accumulation of

density at the imine nitrogens and more charge at the other nitrogens and the carbons.

Finally, consider the effect of deorthogonalization of the CNDO/2 π MO's. Earlier we found that the transformation had little effect on the π -electron dipole moment. But the dipole moment is the expectation value of all these electrons. Looking at Figure 11, we see extensive reapportionment of the π electrons. Electrons are shifted away from the atomic centers into regions between the bonded atoms, just as in the case of the σ electrons (Figure 7). In addition, the π electrons are moved into the transannular regions.

Summary and Conclusions

Dipole moments and electron density maps have been determined from three valence-electron methods in order to elucidate the characteristics of the methods and to gain an understanding of the electronic effects operative in adenine. Transforming the CNDO/2 LCAO–MO coefficients to a nonorthogonal basis shifts both σ and π density into the bonding and lone-pair regions of the molecule. Deorthogonalization also polarizes the charge distribution around the atoms to increase the atomic moments, but renders the total dipole moment in no more favorable agreement with the accepted value. The exaggeration of charge separation in EH theory is clearly revealed in both the dipole moment and electron density calculations. On the other hand, the CNDO/2 scheme gives the least reasonable density maps because of complete neglect of differential overlap. Considering the dipole moments and electron density maps together, the CNDO/2D procedure appears to produce the most reasonable description of adenine's electronic structure.

Acknowledgment. The author is grateful to M. M. Marsh for encouragement and advice.